QUANTUM PHENOMENA AND SHAPE DYNAMICS

by

Furkan Semih Dündar

B.S., Physics, İhsan Doğramacı Bilkent University, 2012

M.S., Physics, Middle East Technical University, 2014

Submitted to the Institute for Graduate Studies in
Science and Engineering in partial fulfillment of
the requirements for the degree of
Doctor of Philosophy

Graduate Program in Physics

Boğaziçi University

2018

QUANTUM PHENOMENA AND SHAPE DYNAMICS

APPROVED BY:

Assoc. Prof. Dr. Levent Akant (Thesis Supervisor)	.....
Prof. Dr. Metin Arık (Thesis Co-supervisor)	.....
Assoc. Prof. Dr. Aşkın Ankay	.....
Assoc. Prof. Dr. A. Savaş Arapoğlu	.....
Assist. Prof. Dr. Gülhan Ayar	.....
Prof. Dr. Enise Nihal Ercan	.....

DATE OF APPROVAL: 25.10.2018

ACKNOWLEDGEMENTS

Furkan Semih Dündar is grateful to Tim Koslowski, Mikhail Sheftel, Edward Anderson, Soley Ersoy, Bayram Tekin, Zahra Mirzaiyan, Medine İldeş, Cihan Pazarbaşı, Erol Barut and Deniz Yılmaz for useful discussions. A special thank goes to my advisor Levent Akant and my co-advisor Metin Arık. Furkan Semih Dündar has been supported by TÜBİTAK 2211A Scholarship. My research is partly supported by the research grant from Boğaziçi University Scientific Research Fund (BAP), research project No. 11643.

ABSTRACT

QUANTUM PHENOMENA AND SHAPE DYNAMICS

In this thesis, we considered quantum phenomena (Unruh effect) in Shape Dynamics, version of Bohmian Mechanics that is compatible with Mach's Principle, and a solution (gravitational collapse of a spherically symmetric thin shell of dust) of Shape Dynamics.

First, it is interesting that we proved the existence of Unruh radiation in Shape Dynamics where there is no Lorentz symmetry and no unbounded flat space. In order to detect the existence of Unruh effect we used an Unruh-DeWitt detector.

Second, a toy model for Shape Dynamics that is suitable for particle interactions is considered. It brings three constraints for solutions: Energy constraint, angular momentum constraint and dilational momentum constraint. We applied these constraints to particle variables of Bohmian Mechanics and obtained a constrained Bohmian Mechanics that is Machian.

Third, we considered a spherically symmetric thins shell of dust in Shape Dynamics in a space manifold which is $[0, 1] \times S^2$. We calculated the symplectic form and its inverse. The phase space variables turned out to be the coordinate radius and total momentum of the shell, the expectation value of the trace of the metric momentum, and the volume of the space. We laid the foundations for future research.

ÖZET

KUANTUM OLGULAR VE ŞEKİL DİNAMİĞİ

Bu tezde Şekil Dinamiği çerçevesinde çeşitli kuantum olguları (Unruh etkisi), Bohm Mekaniğinin Mach ilkesiyle uyumlu bir versiyonunu ve Şekil Dinamiğinin bir çözümünü (Küresel simetrik ince toz kabuğun kütleçekimsel çökmesi) inceledik.

Birinci olarak, ilginçtir ki Unruh etkisini Lorentz simetrisi ve sınırsız uzayan düz uzay olmayan bir çerçevede bulduk. Unruh etkisinin varlığını ise bir Unruh-DeWitt detektörü kullanarak ispat ettik.

İkinci olarak, Şekil Dinamiğinin parçacık etkileşimleri için öne sürülen bir oyuncak modelini ele aldık. Bu kuram üç tane şart getiriyor: Enerji şartı, açısal momentum şartı ve genleşme (dilational) momentumu şartı. Biz de bu şartları Bohm Mekaniğinde parçacık değişkenlerine uygulayarak Bohm Mekaniğinin Mach İlkesiyle uyumlu hale getirdik.

Üçüncü olarak, Şekil Dinamiğinde küresel simetrik ince bir toz kabuğun çöküşünü ele aldık. Buradaki uzaysal manifoldumuz $[0, 1] \times S^2$ oldu. Bu çerçevede simplektik formu ve onun tersini hesapladık. Faz uzayı değişkenleri şu şekilde çıktı: kabuğun koordinat yarıçapı ve toplam momentumu, uzayın hacmi ve metrik momentumun izinin uzaydaki beklenen değeri. Bu sayede ileriki araştırmalar için bir zemin hazırlamış olduk.

TABLE OF CONTENTS

LIST OF FIGURES

LIST OF TABLES

LIST OF SYMBOLS

g_{ab}	Three dimensional Riemannian metric
$g_{\mu\nu}$	Space-time metric of various dimensions with Lorentzian signature
p^{ab}	Conjugate momentum of three dimensional Riemannian metric
$\mathbb{R}^*$	The set of nonzero real numbers
$\mathbb{R}^+$	The set of positive real numbers

LIST OF ACRONYMS/ABBREVIATIONS

BFT	Bohmian Field Theory
BM	Bohmian Mechanics
GR	Einstein's Theory of General Relativity
JBSD	Jualian Barbour's Toy Model for Shape Dynamics
QFT	Quantum Field Theory
SD	Shape Dynamics
SR	Einstein's Theory of Special Relativity

1. INTRODUCTION

Julian Barbour was first to put forward the idea of Shape Dynamics (SD) (which is a theory of gravitation and is simply summarized in [3]) and then its connection with Einstein's General Relativity (GR) was made by other researchers [4–8]. Interested readers may consult to Ref. [9] for a decent review of SD. The Shape Dynamics has the same reduced configuration space as General Relativity but contains a different gauge group. Shape Dynamics's gauge group is local scale (Weyl) transformations whereas in GR there is local Lorentz symmetry. See Table 1.1 for correspondence of concepts used in GR and SD.

In this thesis, we investigated quantum phenomena in the context of SD. Since Lorentz symmetry is inherent in Quantum Field Theory (QFT) we could not use it. Instead we used a field theoretic generalization of Bohmian Mechanics (BM) [10–13] which is called as Bohmian Field Theory (BFT) [14–22].

In Chapter 2 we proved the existence of Unruh effect in a Shape Dynamics background. For that we used a 3-torus as our compact and without boundary space manifold (which is flat) and on the quantum side we used Bohmian Field Theory and an Unruh-DeWitt detector. Because the coupling of the Unruh-DeWitt detector to the interaction Hamiltonian is unknown in the literature, we could only prove the *existence* of the Unruh effect, not its spectrum.

Table 1.1. A summary of concepts used in GR and SD. Here "diff. inv" means diffeomorphism invariance.

General Relativity	Shape Dynamics
4D Space-time	3D Conformal space
4D Diff. invariance	3D Diff. invariance
Local Lorentz symmetry	Local scale symmetry

In Chapter 3 we imposed the constraints of a Shape Dynamics theory that is suitable for particle interactions to Bohmian Mechanics. When these constraints are imposed the Bohmian Mechanics has become Machian and the use of Newton's absolute space-time is allowed.

The phrase "Shape Dynamics" is due to Julian Barbour's investigation [3] of N-body problem under Newtonian gravitational force using only the *shapes* of the configuration as the physically relevant data. There, Barbour considered the configuration space Q^N of N-bodies. Then he quotiented this set by the group TRS (translations, rotations, and scale transformations) and considered elements that can be mapped to each other via this group to be physically same. The quotient space Q^N/TRS was named as the *shape space*. The name *shape* refers to the fact that in order to define a *shape* one only needs the angles between particles.

The introduction of a kinematic metric on shape space and a principle called *best matching* was used to generate dynamics. However with pure relational data, the equations of motion should be third order differential equations. He proposed some constraints: the total momentum of the universe should vanish, the total angular momentum of the universe should vanish, the dilational momentum of the universe vanish (this is the time derivative of the moment of inertia) ,the total energy of the universe should vanish. This way, he could obtain equations of motion that are second order differential equations. We will call the theory of particle interactions in terms of shapes that was put forward in Ref. [3] as Julian Barbour's Toy Model for Shape Dynamics (JBSD). See Appendix B for a rather detailed account of this toy model.

In refs. [4–6] a theory was put forward that contains local scale symmetry instead of GR's local Lorentz symmetry and it has also been called as Shape Dynamics. In this thesis, the theory Shape Dynamics refers to these latter works. This Shape Dynamics as it is understood today has come out of refs. [7, 8]. There the authors used a linking theory approach. They first enlarged the phase space of GR with a scalar field, and then used a constraint to obtain SD. Let us now summarize this work.

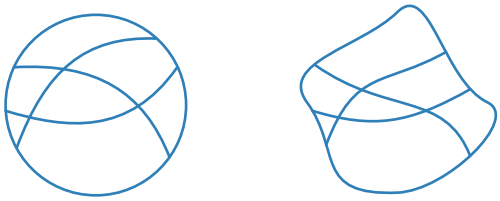

Figure 1.1. SD is invariant under volume preserving conformal transformations. Conformal transformations preserve the angles between the curves in space.

In our introduction of SD we follow [9] and begin with the ADM formalism of GR:

$$\mathcal{H} = \frac{1}{\sqrt{g}}(p^{ab}p_{ab} - \frac{1}{2}p^2) - \sqrt{g}R = 0 \tag{1.1}$$

$$\mathcal{H}^a = -2\nabla_b p^{ab} = 0 \tag{1.2}$$

where $\mathcal{H}$ is the Hamiltonian constraint and $\mathcal{H}^a$ is the three dimensional diffeomorphism constraint. When written in 3+1 Hamiltonian formalism, GR is a constrained system (for more, please see Ref. [23]). We extend the phase space with a scalar function $\phi(x)$ and put the constraint:

$$Q = \pi \approx 0. \tag{1.3}$$

When $\phi(x) \approx 0$ we obtain GR in ADM formalism. Here π is the conjugate momentum of ϕ. Now we make a contact transformation using the following type-2 generating functional:

$$F = \int d^3x \left(g_{ab} P^{ab} + \phi \Pi + g_{ab} (e^{4\hat{\phi}} - 1) P^{ab} \right) \tag{1.4}$$

with

$$\hat{\phi}(x) \equiv \phi(x) - \frac{1}{6} \log \langle \sqrt{g} e^{6\phi} \rangle \tag{1.5}$$

where $\langle f \rangle \equiv \int d^3x f / \int d^3x \sqrt{g}$ is the volume average of f. The result of the transformation are as follows [9]:

$$\frac{\delta F}{\delta g_{ab}} = e^{4\hat{\phi}} P^{ab} + \frac{1}{3} (e^{6\hat{\phi}} - 1) \langle e^{4\hat{\phi}} g_{cd} P^{cd} \rangle \sqrt{g} g^{ab} \tag{1.6}$$

$$\frac{\delta F}{\delta \phi} = \Pi + 4 \left(e^{4\hat{\phi}} g_{cd} P^{cd} - \langle e^{4\hat{\phi}} g_{cd} P^{cd} \rangle \sqrt{g} e^{6\hat{\phi}} \right) \tag{1.7}$$

$$\frac{\delta F}{\delta \Pi^{ab}} = e^{4\hat{\phi}} g_{ab} \tag{1.8}$$

$$\frac{\delta F}{\delta \Pi} = \phi. \tag{1.9}$$

These rules let us write new coordinates in the enlarged phase space as follows [9]:

$$P^{ab} = e^{-4\hat{\phi}} \left[p^{ab} - \frac{1}{3}(1 - e^{6\hat{\phi}})\langle p \rangle \sqrt{g} g^{ab} \right] \tag{1.10}$$

$$\Pi = \pi - 4(p - \langle p \rangle \sqrt{g}) \tag{1.11}$$

$$G_{ab} = e^{4\hat{\phi}} g_{ab} \tag{1.12}$$

$$\Phi = \phi. \tag{1.13}$$

The constraints of the linking theory are [9]:

$$\mathcal{H}_{\hat{\phi}} = \frac{e^{-6\hat{\phi}}}{\sqrt{g}} \left(p_{ab} p^{ab} + \frac{1}{3} \left(1 - e^{6\hat{\phi}} \right) \langle p \rangle p - \frac{1}{6} g \left(1 - e^{6\hat{\phi}} \right)^2 \langle p \rangle^2 - \frac{p^2}{2} \right) \tag{1.14}$$

$$- \sqrt{g} \left(R e^{2\hat{\phi}} - 8 e^{\hat{\phi}} \nabla^2 e^{\hat{\phi}} \right) \approx 0 \tag{1.15}$$

$$\mathcal{H}^a_{\hat{\phi}} = -2 e^{-4\hat{\phi}} \left[\nabla_b p^{ab} - 2(p - \sqrt{g}\langle p \rangle) \nabla^a \phi \right] \approx 0 \tag{1.16}$$

$$\mathcal{Q}_{\hat{\phi}} = \pi - 4(p - \sqrt{g}\langle p \rangle) \approx 0. \tag{1.17}$$

In order to obtain constraints for SD, we set $\pi \approx 0$:

$$\mathcal{H}_{\hat{\phi}} = \frac{e^{-6\hat{\phi}}}{\sqrt{g}} \left(p_{ab} p^{ab} + \frac{1}{3} \left(1 - e^{6\hat{\phi}} \right) \langle p \rangle p - \frac{1}{6} g \left(1 - e^{6\hat{\phi}} \right)^2 \langle p \rangle^2 - \frac{p^2}{2} \right) \tag{1.18}$$

$$- \sqrt{g} \left(R e^{2\hat{\phi}} - 8 e^{\hat{\phi}} \nabla^2 e^{\hat{\phi}} \right) \approx 0 \tag{1.19}$$

$$\mathcal{H}^a_{\hat{\phi}} = \nabla_b p^{ab} \approx 0 \tag{1.20}$$

$$\mathcal{Q}_{\hat{\phi}} = p - \sqrt{g}\langle p \rangle \approx 0. \tag{1.21}$$

For a summary of the process see Figure 1.2.

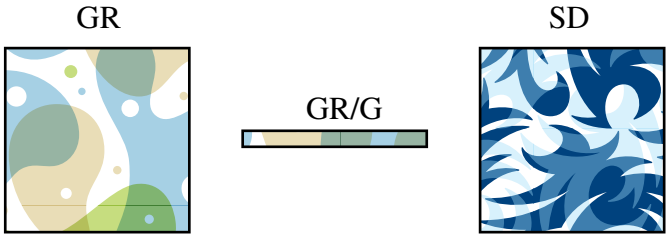

Figure 1.2. A graphical summary of the linking theory approach: the configuration space of GR is quotiented by the gauge group G (local Lorentz symmetry) and then is added local scale symmetry (Weyl symmetry) in order to obtain SD.

1.1. A Birkhoff's Theorem for Shape Dynamics

In Einstein's General Theory of Relativity, Birkhoff theorem states that the spherically symmetric vacuum solution of Einstein field equations in an asymptotically flat space-time is the Schwarzschild solution. It is represented as follows:

$$ds^2 = -\left(1 - \frac{2M}{r}\right) dt^2 + \left(1 - \frac{2M}{r}\right) dr^2 + r^2(d\theta^2 + \sin^2\theta d\phi^2). \tag{1.22}$$

Similar to this solution, Henrique Gomez investigated the applicability of Birkhoff's heorem in a Shape Dynamics background [24]. We will only give the result of his analogue Birkhoff's Theorem for the Shape Dynamics with an open space manifold. For details the readers may consult to Ref. [24].

Theorem 1.1 (Birkhoff's Theorem for Shape Dynamics [24])**.** *Given the following asymptotically flat conditions:*

$$g_{ab} \to \delta_{ab} + \mathcal{O}(r^{-1}) \tag{1.23}$$

$$\pi^{ab} \to \mathcal{O}(r^{-2}) \tag{1.24}$$

$$N \to 1 + \mathcal{O}(r^{-1}) \tag{1.25}$$

$$\xi^a \to \mathcal{O}(1) \tag{1.26}$$

the only solution of the field equations (Equations (4), (9), (10), (11) in Ref. [24]) can be given by the following line element in 4D:

$$ds^2 = -\left(\frac{1-\frac{M}{2r}}{1+\frac{M}{2r}}\right)^2 dt^2 + \left(1+\frac{M}{2r}\right)^4 (dr^2 + r^2 d\Omega^2). \tag{1.27}$$

Here g_{ab} is the 3-metric, π^{ab} is its conjugate momentum, N is the lapse function and finally ξ^a is the shift vector. The actual theorem refers to more variables to denote the solution but we have given here the essence of it.

Last but not least, let us add an interesting note that the spherically symmetric vacuum solution of SD is not a black hole but a worm hole. See Figure 1.3. It consists of the space-time patches that is covered by the Schwarzschild solution of GR in isotropic coordinates.

1.2. Classical Firewalls?

In order to understand the comments about the classical firewalls in Shape Dynamics, we need to go over the details of firewalls in quantum gravity; which we do in the next subsection.

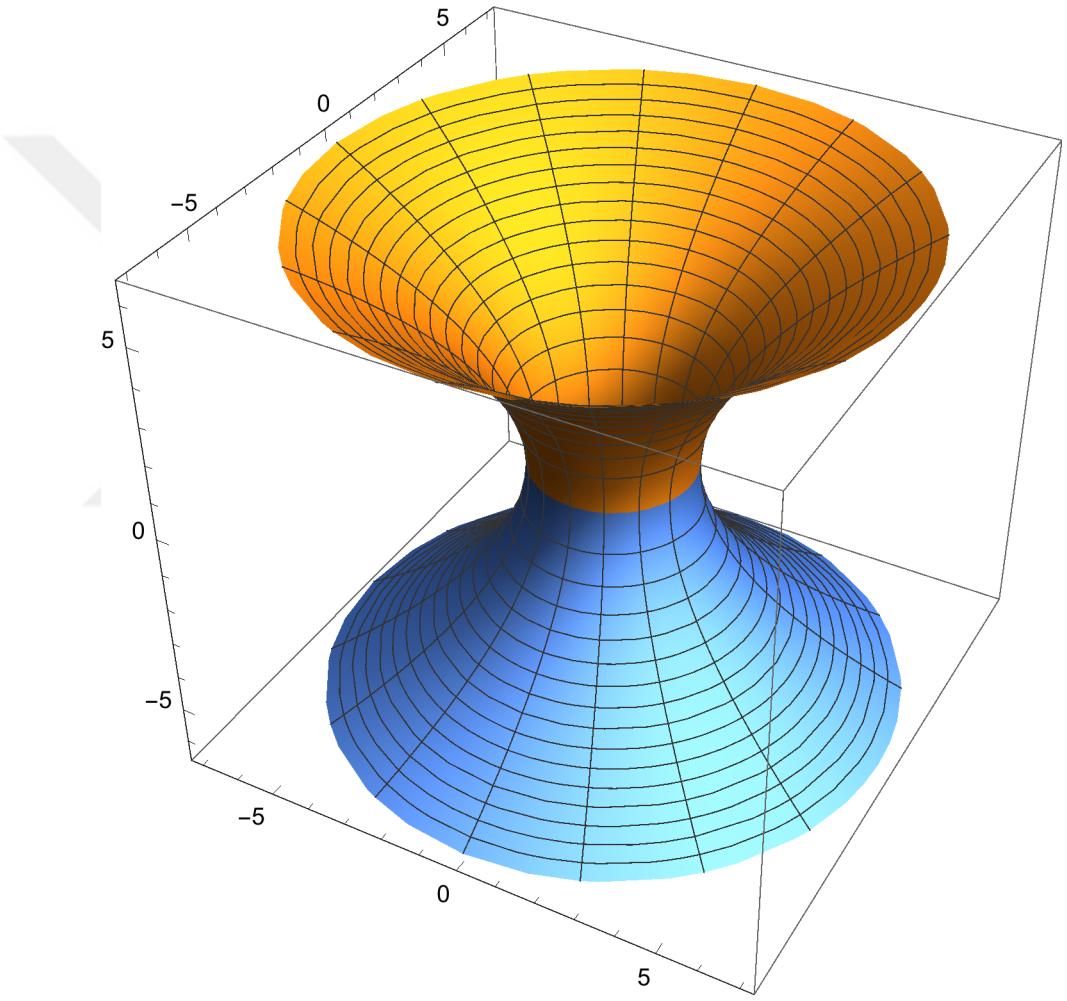

Figure 1.3. Constant t and $\theta = \pi/2$ slice of the space-time.

1.2.1. Firewalls in Quantum Gravity

We would like to note that there is a comprehensive Master of Science thesis of the author [1]. We will briefly summarize the main arguments behind the firewall paradox and refer the interested readers to Ref. [1]. We will closely follow this reference.

In order to understand the firewall paradox, we need to briefly go over the details of black hole complementarity (BHC) [25]. BHC has been put forward to solve the xeroxing paradox in black hole evaporation.

According to the laws of quantum mechanics, an arbitrary quantum state cannot be copied. This is known in the physics literature as the *No-Cloning Theorem*. Let us give a simple proof (for a more detailed proof using the 'Generalized Measurement Approach' one may see the Appendix of Ref. [1]).

Let us consider a two-level system with eigenstates $|+\rangle, |-\rangle$, and a *quantum cloning operator* L. The action of L on $|+\rangle$ is given as follows:

$$L|+\rangle = |+\rangle \otimes |+\rangle. \tag{1.28}$$

However when we consider a superposed state such as $(|+\rangle + |-\rangle)/\sqrt{2}$, we obtain a contradiction. There are two ways to calculate the action of the quantum cloning operator on this superposed state. First is to act on the state as a whole, the second is to act its parts using the linearity of quantum operators.

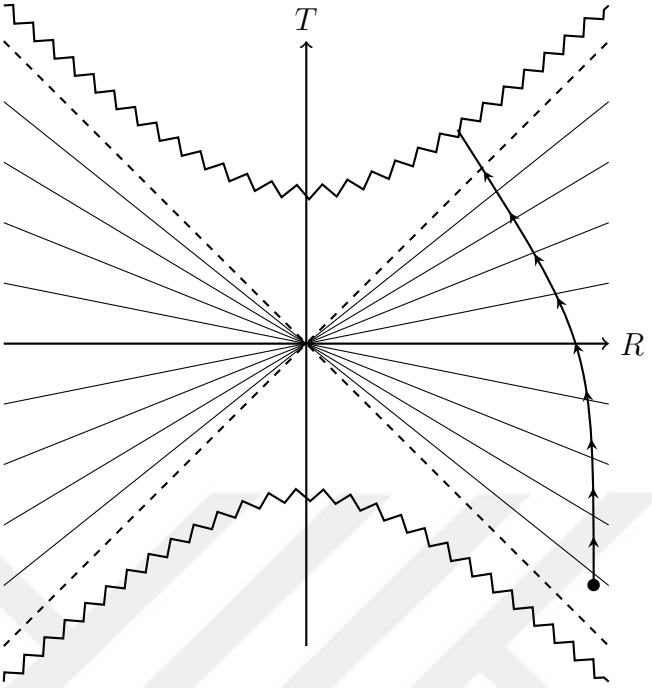

Figure 1.4. A possible trajectory for a qubit is drawn in a Kruskal diagram of a maximally extended Schwarzschild solution. Constant t hypersurfaces are depicted with straight lines. The observer well outside the black hole never sees the qubit passing the event horizion. [1].

$$L\frac{|+\rangle + |-\rangle}{\sqrt{2}} = \frac{1}{2}(|+\rangle + |-\rangle) \otimes (|+\rangle + |-\rangle) \tag{1.29}$$

$$L\frac{|+\rangle + |-\rangle}{\sqrt{2}} = \frac{1}{2}(|+\rangle \otimes |+\rangle + |-\rangle \otimes |-\rangle). \tag{1.30}$$

As one sees the two ways of calculating the same procedure does not give the same answers. Hence, quantum cloning for arbitrary states is not possible.

Now, consider black holes. When we throw a qubit inside a, for example, Schwarzschild black hole it hits the singularity. However, according to a observer standing well outside the black hole, it reaches the event horizon ($r \to 2M^+$) and never crosses it. This is relativity. See Figure 1.4.

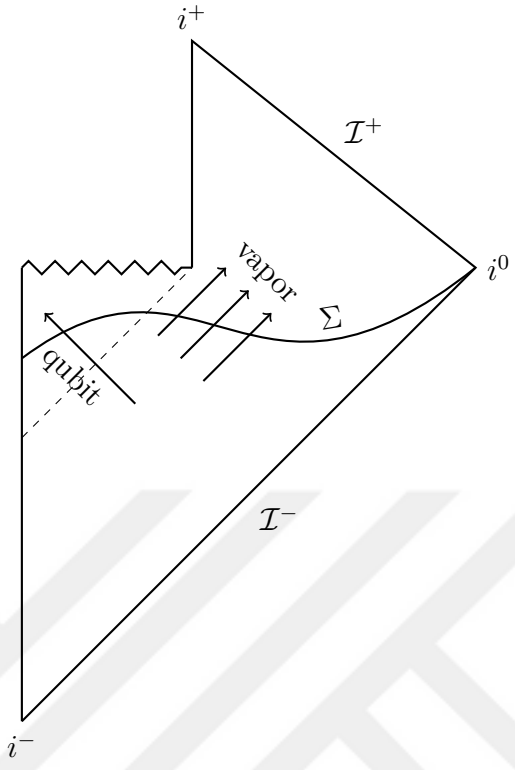

Figure 1.5. The information of the qubit that falls into a black hole is both inside and outside of the black hole [1].

The BHC considers a stretched horizon just a single Planck area bigger than the event horizon as the surface where all the particles that fall into black hole condensates.

When the black hole evaporates unitarily, the information of the fallen qubit should be found in the black hole vapor. The (arbitrary) qubit is both inside and outside of the black hole, and it is cloned! See Figure 1.5. This must be forbidden by quantum mechanics. The BHC comes into play at this moment. It postulates three ideas [25]:

(i) The process of formation and evaporation of a black hole, as viewed by a distant observer, can be described entirely within the context of standard quantum theory. In particular, there exists a unitary S-matrix which describes the evolution from infalling matter to outgoing Hawking-like radiation.

(ii) Outside the stretched horizon of a massive black hole, physics can be described

to good approximation by a set of semiclassical field equations.

(iii) To a distant observer, a black hole appears to be a quantum system with discrete energy levels. The dimension of the subspace of states describing a black hole of mass M is the exponential of the Bekenstein entropy $S(M)$.

The information of the qubit is both inside and out side of the stretched horizon. Its location differs according to whether the observer is inside or outside of the black hole. BHC [25] proves that if an outside observer distills the information carried by the qubit from the Hawking radiation and decides to dive into the black hole, he never encounters the qubit inside the black hole. Therefore the xeroxing paradox is resolved in operational terms.

The paper that introduced the firewall paradox [26] which was written by Ahmed Almheiri, Donald Marolf, Joseph Polchinski and James Sully (AMPS), highlights the hidden fourth postulate of BHC: It is the equivalence principle.

(iv) A freely falling observer experiences nothing out of the ordinary when crossing the horizon.

Let us talk more about quantum mechanics first. Don Page considered a two-partite finite dimensional Hilbert space, $H_M \otimes H_R$ [27] (In our case, H_M is the black hole Hilbert space, and H_R is the Hilbert space of the Hawking radiation). He considered random states in this big Hilbert space. He found out that when the degrees of freedom in H_M is less than H_R, the random quantum pure state is maximally entangled[1] . Keep this in mind, it will be important.

Because the energy radiated away by the black hole is finite, AMPS thought that the calculation of Don Page can be used for an evaporating black hole. AMPS considered an *old* black hole, meaning that it radiated away half of its degrees of

[1]Let us give the definition of a maximally entangled state as a side note [28]: "The meaning of maximal entanglement is that for every observable in A, one can predict the result of measuring it by measuring the corresponding observable in B. In a maximally entangled state the density matrix of A is proportional to the identity ..."

freedom. Therefore the black hole is maximally entangled with the early Hawking radiation.

Let us consider a newly emitted Hawking particle from an old black hole. If the equivalence principle is valid, it should be maximally entangled with the black hole. On the other hand, because it was a part of black hole degree of freedom, it also must be maximally entangled with the early radiation. However quantum mechanics does not allow a particle to be maximally entangled with two other separate systems (the exact reason is the strong sub-additivity of entropy: In a three-partite system, $H_A \otimes H_B \otimes H_C$,, one must have $S_{AB} + S_{BC} \geq S_B + S_{ABC}$. Here $H_A = H_M$, H_B is the single particle Hilbert state of the newly emitted radiation, and $H_C = H_R$). If we insist that the black hole evaporation is unitary, the particle should be maximally entangled with the early radiation, and not the black hole. This requirement seriously breaks down the quantum vacuum at the event horizon. Therefore the event horizon becomes a firewall: There exist particles of all energy levels at the horizon, it becomes singular; hence the name *firewall*.

1.2.2. Shape Dynamic Horizons: Classical Firewalls?

In this subsection we summarize Section 3.3 (named "Shape Dynamic Horizons: Classical Firewalls?") of Ref. [29]. In Shape Dynamics the Einstein's equivalence principle (iv) is not a fundamental axiom but an emergent property of solutions and it exactly fails down to emerge at the event horizon. The infalling observers therefore can detect whether they crossed the event horizon or not by measuring the volume of a box. Its volume decreases as the observer approaches the event horizon and begins to expand once the event horizon it passed through.

Although the authors of Ref. [29] notes that event horizon of a Shape Dynamics black hole is the place where the equivalence principle breaks down classically, this firewall is not like the firewall we mentioned in the preceeding subsection. The authors of Ref. [29] say that they are considering Shape Dynamics firewalls in the context of quantum Shape Dynamics black holes.

1.3. Last Words for Introduction

So far we have introduced SD. Now let us give details of what is done in the next chapters. In Chapter 2 we give a derivation of the Unruh effect in the space of 3 dimensional torus in SD using BFT (in Appendix A we go over the details of standard Unruh effect in $1+1$ flat space-time). In Chapter 3 we consider a Machian version of Bohmian Mechanics. The connection to Mach's Principle for Bohmian Mechanics is done through Julian Barbour's Toy Model for Shape Dynamics. This toy model, produced three constraints on particle variables in Bohmian Mechanics if Newton's absolute space is to be used. (We go over the details of Julian Barbour's Toy Model for Shape Dynamics in Appendix B).

2. UNRUH EFFECT IN SHAPE DYNAMICS VIA BOHMIAN FIELD THEORY

The work in this Chapter is published in Ref. [30] and we follow it closely.

The standard Unruh effect [31] (see Appendix A) causes accelerating observers to see radiation in the Minkowski vacuum state of quantum fields. In SD, the space is required to be compact and closed. In ref. [32], Unruh radiation in compact space in the context of special relativity has been found. We will go over the details of standard Unruh effect in $1+1$ dimensions in Minkowski space-time and finally in 3 dimensional space in Shape Dynamics.

Unruh effect might seem to require a Minkowski space-time. However, ref. [32] showed the existence of Unruh effect in a compact space. In ref. We found out in [30] Unruh effect in the context of SD via BFT and an Unruh-DeWitt detector. This is an interesting result in a theory (SD) where there is no Lorentz symmetry.

In Chapter 1 we introduced the Shape Dynamics. Here we would like to briefly go over the details of coupling a Bohmian massive scalar field to Shape Dynamics following ref. [33]. Overall, in this section, we will closely follow ref. [30].

Let Σ, N and ξ^a respectively be a compact space, the lapse function and the shift vector field. In the ADM formalism the line element of GR can be written as follows:

$$ds^2 = (g_{ab}\xi^a\xi^b - N^2)dt^2 + 2g_{ab}\xi^a dx^b dt + g_{ab}dx^a dx^b. \tag{2.1}$$

N, ξ^a are the Lagrange multipliers of the following constraints:

$$S(N) = \int_\Sigma d^3x N\Big(\frac{\pi^{ab}(g_{ac}g_{bd} - g_{ab}g_{cd}/2)\pi^{cd}}{\sqrt{g}} - (R - 2\Lambda)\sqrt{g} + \text{matter terms}\Big) \tag{2.2}$$

$$H(\xi) = \int_\Sigma d^3x(\pi^{ab}\mathcal{L}_\xi g_{ab} + \pi^A\mathcal{L}_\xi\phi_A) \tag{2.3}$$

where ϕ_A and π^A are matter fields and their conjugate momenta. Time evolution is generated by $S(N)+H(\xi)$. In the CMC gauge of GR ($\pi - \langle\pi\rangle\sqrt{g} = 0$), the conformal factor Ω_0 solves the Lichnerowicz-York (LY) equation:

$$8\nabla^2\Omega = R\Omega + \left(\frac{\langle\pi\rangle^2}{6} - 2\Lambda\right)\Omega^5 - \frac{1}{g}\Omega^{-7}\sigma^{ab}\sigma_{ab} + \text{matter terms} \tag{2.4}$$

where $\sigma^{ab} \equiv \pi^{ab} - \pi g^{ab}/3$ is the traceless conjugate momentum of the metric. It turns out that the York Hamiltonian, $\int_\Sigma d^3x\sqrt{g}\Omega_0^6$, generates time evolution in York time, $\tau = 2\langle\pi\rangle/3$ where $\pi = \pi^{ab}g_{ab}$ and $\langle\pi\rangle = \int_\Sigma \pi / \int_\Sigma \sqrt{g}$. The smeared gauge-fixing condition

$$Q(\rho) = \int_\Sigma d^3x\rho\left(\pi - \frac{3}{2}\tau\sqrt{g}\right) \tag{2.5}$$

functions "as a generator of spatial conformal transformation for the metric and the trace-free part of the metric momenta and forms a closed constraint algebra with the spatial diffeomorphism generator" [33]. Therefore the gauge-fixing condition (2.5)

can be used to map $\pi \to \frac{3}{2}\tau\sqrt{g}$ and from now on τ becomes an "abstract evolution parameter" [33] and the total volume of space, $V = \int_\Sigma d^3x\sqrt{g}$, is pure gauge. This new theory is called as shape dynamics with the Hamiltonian

$$H_{SD} = \int_\Sigma d^3x\sqrt{g}\Omega_0^6[g_{ab}, \pi^{ab} \to \sigma^{ab} + \frac{3}{2}\tau g^{ab}\sqrt{g}, \phi_A, \pi^A]. \tag{2.6}$$

In order to better understand the relation of SD to GR, readers may see refs. [7,8] which use the linking theory approach.

2.1. Classical massive scalar field on a shape dynamics background

We begin with a massive scalar field on SD. The required steps to follow have already been sketched in [33] and we will follow them closely. We require two properties: 1) perturbation theory is valid and 2) we look for description on short time intervals. The former one is needed to use the perturbation theory and the latter is to neglect the back-reaction of the field on space.

It is assumed that the Hamiltonian, H_{SD}, is even in field quantities, and can be expanded perturbatively $H_{SD} = H_0 + \varepsilon H_1 + \mathcal{O}(\varepsilon^2)$. Let ϕ and ϖ be the massive scalar field and its conjugate field momentum and $\Omega = \Omega_0 + \varepsilon\Omega_1 + \mathcal{O}(\varepsilon^2)$ be the solution of the LY equation (2.4), where Ω_0 solves the source-free LY equation. We expand the LY equation perturbatively in ε and the result to first order is the following:

$$\Omega_1 = \int_\Sigma d^3y K(x,y)\frac{H^{quad}_{matt}}{\Omega_0\sqrt{g}}(y) \tag{2.7}$$

where H^{quad}_{matt} is quadratic in the field, ϕ, and its momenta and $K(x,y)$ is the Green's function given by:

$$K(x,y) = \left[8\nabla^2 - \left(R + 5(\frac{3}{8}\tau^2 - 2\Lambda)\Omega_0^4 + \frac{\sigma^{ab}\sigma_{ab}}{g}\Omega_0^{-8}\right)\right]^{-1} \tag{2.8}$$

where we used $\tau = 2\langle\pi\rangle/3$. For a massive scalar Bohmian field, the following is valid:

$$H^{quad}_{matt} = \frac{1}{2}\left(\frac{\varpi^2}{\sqrt{g}} + (\Omega_0^4 g^{ab}\partial_a\phi\partial_b\phi + m^2\phi^2)\sqrt{g}\right). \tag{2.9}$$

On the other hand, the first order Hamiltonian, H_1, is given as follows:

$$H_1 = 6\int d^3x\, d^3y \sqrt{g}(x)\Omega_0^5(x)K(x,y)H^{quad}_{matt}(y). \tag{2.10}$$

Because the lapse function, $N(x)$, is the Lagrange multiplier of the Hamiltonian, we obtain:

$$N(y) = 6\int_\Sigma d^3x\ \sqrt{g}(x)\Omega_0^5(x)K(x,y). \tag{2.11}$$

2.2. Uniformly accelerating observers and shape dynamics variables

From now on, we will consider a constantly accelerating observer. The four dimensional Rindler metric for the observer in SR is the following:

$$ds^2 = -e^{2a\xi}d\lambda^2 + e^{2a\xi}d\xi^2 + dy^2 + dz^2. \tag{2.12}$$

When looked at from the perspective of ADM formalism, there is no shift vector, and the Lapse function is as $N = e^{a\xi}$ whereas the three dimensional metric is given by:

$$g_{ab} = \text{diag}(e^{2a\xi}, 1, 1). \tag{2.13}$$

The compact manifold considered for SD is a three torus Σ with side lengths L_x, L_y and L_z and with volume $V = \prod_i L_i$. See Figure 2.1. The coordinate change required in order to move to Σ with Cartesian coordinates is $e^{a\xi}d\xi \to dx$. Hence if x ranges from 0 to L_x, ξ has a range from $-\infty$ to $L_\xi = \ln(aL_x)/a$.

In Rindler space p^{ab} vanishes. The Hamiltonian constraint (2.2) is automatically satisfied as well as the diffeomorphism constraint (2.3) because the lapse function is zero. On the other hand, the first order LY equation (2.4) becomes $\nabla^2\Omega_0 = 0$. We choose $\Omega_0 = 1$ as a solution.

It is quite easy to solve equation (2.8) for $K(x, y)$ under these circumstances. It is proportional to the Green's function for the Laplacian on 3-torus. However there is a subtlety in tori in terms of the Green's function equation [34]. For example, the equation to be satisfied by the Green's function on 3-torus with volume V is [30]:

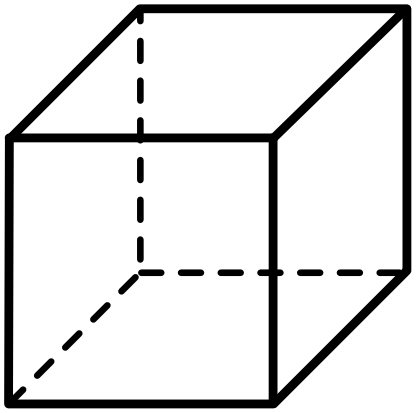

Figure 2.1. Three torus we use as our compact space Σ. The side lengths are L_x, L_y and L_z with total volume $V = \prod_i L_i$. Opposite faces of the cube are identified with each other.

$$\nabla_x^2 G(\vec{x}, \vec{y}) = \delta(\vec{x} - \vec{y}) - \frac{1}{V} \tag{2.14}$$

where the volume term is required for consistency[2] . In this case, $K(x, y)$ is:

$$K(x, y) = \frac{1}{8|\vec{x} - \vec{y}|} - \frac{|\vec{x} - \vec{y}|^2}{48V}. \tag{2.15}$$

The first term in equation (2.15) might be replaced by its principle value so as to avoid a singularity at $\vec{x} = \vec{y}$. This solution is valid in Cartesian coordinates in Σ. What is more, "this is valid when the average value of $\sqrt{|g|}H_{matt}^{quad}$ over space is zero. Otherwise

[2]The consistency requirement is as follows: Let us integrate Equation (2.14) in a space that has no boundary but has finite volume. The left hand side of the equation will yield zero after using the Gauss' Theorem, since the manifold has no boundary. On the other hand, the right hand side of the equation will not be zero unless there is a $1/V$ term. This is the reason why the inclusion of $1/V$ term on the right hand side in Green's equation is necessary for consistency in a manifold that has no boundary but has finite volume.

the Laplace equation is not invertible on compact spaces without boundary" [30].

2.3. A Brief Account of Bohmian Mechanics and Bohmian Field Theory

Bohmian Mechanics (BM) is a realistic interpretation of the standard quantum mechanics (*i.e.* Copenhagen interpretation) [10–13]. The exact positions of particles are the hidden variables of Bohmian Mechanics. It can be said that it is a nonlocal hidden variables theory. In Bohmian Mechanics, there are two pillars: The wavefunction, and the particle positions. The time evolution of the wavefunction is given by the Schrödinger equation [10]:

$$i\hbar\frac{\partial\Psi}{\partial t} = H\Psi. \tag{2.16}$$

On the other hand, the velocity of each particle is a function of the probability current [10] (see Appendix C for a derivation of the probability current in quantum mechanics):

$$\vec{v}_k = \frac{\hbar}{m_k}\frac{\Im(\Psi^*\nabla_k\Psi)}{|\Psi|^2} \tag{2.17}$$

where k runs through the particle numbers and $\Im(\cdot)$ is the imaginary part of the term inside the parenthesis. Note that the Equation (2.17) is a first order differential equation. Therefore the particle paths never cross each other.

Bohmian Field Theory (BFT) [15] is a stochastic field theory. The path that is traced by the system in the configuration space (Q) is a piece-wise continuous curve. When particles are emitted or absorbed jumps occur in the piece-wise continuous curve

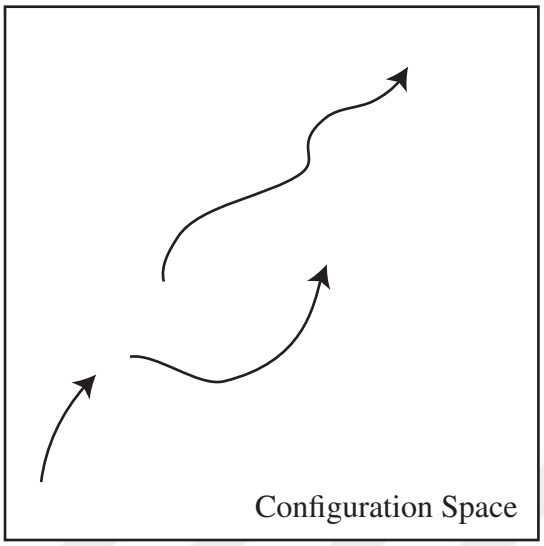

Figure 2.2. When particles are emitted or absorbed in BFT, the continuity of the curve in the configuration space breaks down and jumps occur.

[15]. See Figure 2.2. Let us write the total Hamiltonian of the system as $H = H_0 + H_I$ "where H_0 is the free Hamiltonian and H_I is the interaction Hamiltonian" [30]. In the continuous part of the path in the configuration system the configuration evolves as in the following formula [15]:

$$\frac{dQ_t}{dt} = \Re \frac{\Psi_t^*(Q_t)(\hat{\dot{q}}\Psi_t)(Q_t)}{|\Psi_t(Q_t)|^2} \tag{2.18}$$

where $\Re(x)$ expresses the real part of x and

$$\hat{\dot{q}} = \frac{d}{dt} e^{iH_0 t} \hat{q} e^{-iH_0 t} = i[H_0, \hat{q}]. \tag{2.19}$$

The wave-function $\Psi_t(q)$ evolves in time according to the time dependent Schrödinger equation. If a jump occur, $\sigma^{\Psi}(dq|q')$ denotes the transition rate in dt seconds from a point q' in configuration space to a volume element dq around a point q in the configuration space [15]:

$$\sigma^{\Psi}(dq|q') = 2\frac{[\Im\Psi^*(q)\langle q|H_I|q'\rangle\Psi(q')]^+}{|\Psi(q')|^2} \tag{2.20}$$

where $\Im(x)$ expresses the imaginary part of x and x^+ expresses the positive part of x, that is $x^+ = \max(x, 0)$.

2.4. Massive scalar Bohmian field on a shape dynamics background and the Unruh effect

We consider a Bohmian field in the Schrödinger wavefunctional picture. Because the Hamiltonian is time-independent, we have:

$$\int_\Sigma H^{quad}_{matt}\Psi = \int_\Sigma \frac{1}{2}\left(-\frac{\delta^2}{\delta\phi^2} + |\nabla\phi|^2 + m^2\phi^2\right)\Psi = 0. \tag{2.21}$$

This is the time-independent Schrödinger equation with vanishing energy. This should be the case since the integral $\int_\Sigma H^{quad}_{matt}$ should be equal to zero on a compact space without boundary.

We would like to make use of an Unruh-DeWitt detector to detect the Unruh radiation. Therefore we add a term $-\lambda\chi\theta\phi$ to the Hamiltonian. "λ is a small coupling constant and θ 'is the operator of the detector's monopole moment' [35] and χ is a smooth switching function [36]" [30]. The quadratic Hamiltonian becomes [30]:

$$H_{matt}^{quad} = \frac{1}{2}\left(-\frac{\delta^2}{\delta\phi^2} - \phi\nabla^2\phi + m^2\phi^2\right) - \lambda\chi\theta\phi. \tag{2.22}$$

up to a surface term that vanishes. Hence, the time-independent Schrödinger equation after the addition of an Unruh-DeWitt detector is as follows:

$$\int_\Sigma H_{matt}^{quad}\Psi = \int_\Sigma \left[\frac{1}{2}\left(-\frac{\delta^2}{\delta\phi^2} - \phi\nabla^2\phi + m^2\phi^2\right) - \lambda\chi\theta\phi\right]\Psi = 0. \tag{2.23}$$

The Unruh-DeWitt detector is a two level system with energy levels equal to $E_0 = 0$, $E = -E_1$ where E_1 is a positive quantity. The uncoupled Hamiltonian can have two states with energies $0, E_1$. This is mainly because the total energy should vanish. On the other hand The interaction Hamiltonian H_I is as follows:

$$H_I = 6\int_{\Sigma\times\Sigma} K(x,y)H_{matt}^{quad}(y). \tag{2.24}$$

The transition rate for BFT (2.20) is thus,

$$\sigma^{\Psi} = 2\frac{[\Im\Psi^*(q,t)H_I\Psi(q',t)]^+}{|\Psi(q',t)|^2}. \tag{2.25}$$

So as to calculate the transition rate, we should remind ourselves about the time dependence (e^{-iE_it}) of the wave functionals:

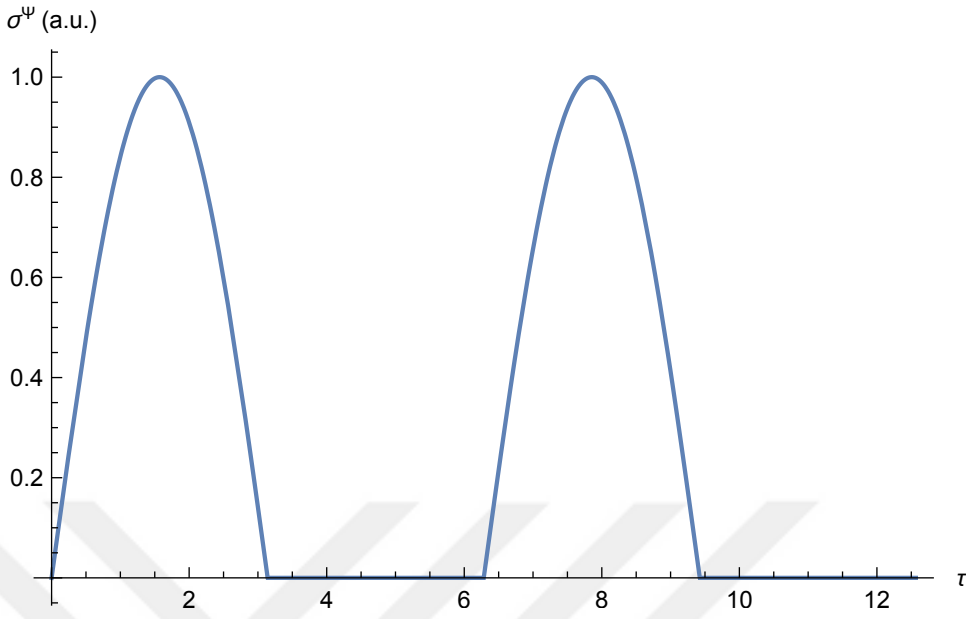

Figure 2.3. The nonzero transition (jump) rate is illustrated when $E_q = E_1$ and $E_{q'} = E_0$. The horizontal axis is scaled such that $\tau = (E_1 - E_0)t = E_1 t$. The vertical axis is σ^Ψ in arbitrary units.

$$\sigma^\Psi = 2\frac{[\Im e^{i(E_q - E_{q'})t}\Psi^*(q)H_I\Psi(q')]^+}{|\Psi(q')|^2} \tag{2.26}$$

$$= 2\frac{\Psi(q)H_I\Psi(q')}{|\Psi(q')|^2}\sin^+(E_1 t). \tag{2.27}$$

Hence it is shown that there is a nonzero jump rate from vacuum to a state with one particle (See Figure 2.3). In the approach we used, the number of field excitations (*i.e.* the number of particles) "is directly related to the number of available states of the Unruh-DeWitt detector. We have been unable to exactly determine the particle production rate, however we have at least shown that there is Unruh radiation detected by Unruh-DeWitt detectors for a Bohmian field theory on a shape dynamics background" [30].

3. BOHMIAN MECHANICS MADE MACHIAN

The work in this Chapter is published in Ref. [37] and we follow it closely including Section 3.1 then look out for some simple solutions of the theory in Section 3.2.

In the physics literature there are at least ten versions of the Mach Principle. Hermann Bondi and Joseph Samuel Ref. [38] give some these versions. They are as follows [38]:

(i) The universe, as represented by the average motion of distant galaxies does not appear to rotate relative to local inertial frames.
(ii) Newton's gravitational constant G is a dynamical field.
(iii) An isolated body in otherwise empty space has no inertia.
(iv) Local inertial frames are so affected by the cosmic motion and distribution of matter that the universe as represented by the average motion of matter does not appear to rotate when viewed from local inertial frames.
(v) The universe is spatially closed.
(vi) The total energy, angular and linear momentum of the universe are zero.
(vii) Inertial mass is affected by the global distribution of matter.
(viii) If you take away all matter, there is no more space.
(ix) $\Omega = 4\pi\rho GT^2$ is a definite number of order unity, where ρ is the mean density matter in the universe and T is the Hubble time.
(x) There are no absolute elements.
(xi) Overall rigid rotations and translations of a system are unobservable.

The version of Mach's Principle we embrace is Julian Barbour's interpretation [39] (see Figure 3.1):

(xii) In order for a theory to be Machian, a tangent vector or a direction in the reduced configuration (configuration space quotiented by the gauge groups) space should be able to determine the evolution of the system uniquely.

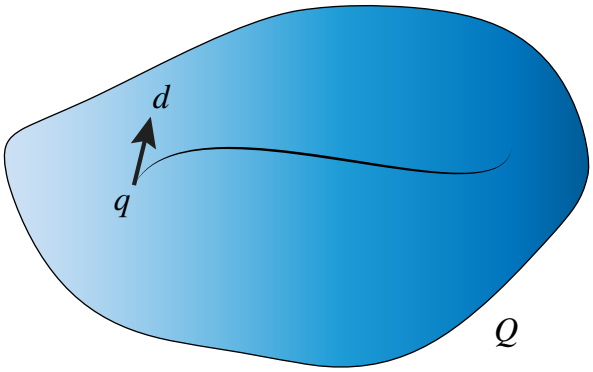

Figure 3.1. A point (q) in reduced configuration space (Q) and a direction (d) or a tangent vector determines the time evolution of the system uniquely.

Shape Dynamics is a Machian theory consistent with the Julian Barbour's interpretation of it [39]. The version of Shape Dynamics we handle here is Julian Barbour's non-relativistic version (JBSD. See Appendix B for a short review) [3]. Why we use this version is that Bohmian Mechanics is also non-relativistic.

In JBSD, the true physical degrees of freedoms are inter-particle separations and the time derivatives of those. For an N-particle system, the number of inner-particle separations is $N(N-1)/2$. On the other hand, in a Newton's absolute space-time there are $3N$ many coordinates in a 3D space. This colossal reduction in the number of variables is why we will investigate our equations in the Newtonian absolute space-time. So as to make a theory Machian in Newton's absolute space-time, JBSD puts with various constraints. Therefore, we can use the Newton's absolute space-time as long as the following constraints are satisfied (we adapted the constraints appearing in Ref. [3] to quantum mechanics):

$$H\Psi = 0 \tag{3.1}$$

$$\sum_k \vec{L}_k \Psi = 0 \tag{3.2}$$

$$\sum_k \vec{r}_k \cdot \vec{p}_k \Psi = 0 \tag{3.3}$$

where $\vec{L}_k = \vec{r}_k \times \vec{p}_k$ and $\vec{p}_k = -i\hbar\vec{\nabla}_k$. These are the energy constraint, the angular momentum constraint and the dilational momentum constraint (Dilational momentum is the time derivative of moment of inertial. One can think of moment of inertia as a measure of the *shape* of the system).

3.1. The Machian Description of Bohmian Mechanics

In this section we modify the constraints of JBSD according to the variables of Bohmian Mechanics and will make Bohmian Mechanics Machian. There is already an exact velocity of a particle in Bohmian Mechanics. By multiplying the velocity with the mass of the particle, we can obtain the exact momentum of that particle. Hence, we will not use the momentum operator, $-i\hbar\vec{\nabla}$. Be aware that, momenta in Bohmian Mechanics are functions of the wavefunction, see Equation (2.17). The wavefunction plays a central role in our description.

Similarly, one can write down the orbital angular momentum of a particle as $m_k\vec{r}_k \times \vec{v}_k$ instead of $\vec{L}_k\Psi$. The Hamiltonian is, as well known, the kinetic energy plus the potential energy. The Hamiltonian constraint can be written down as follows instead of $H\Psi = 0$:

$$H_{BM} = \sum_k \frac{1}{2} m_k v_k^2 + \frac{1}{2}\sum_{k,k'} V(\vec{r}_k, \vec{r}_{k'}) = 0. \tag{3.4}$$

We added a subscript BM to H in order to mark that it is calculated using the particle positions. All in all, the equations of motion in Bohmian Mechanics are the same:

$$i\hbar\frac{\partial\Psi}{\partial t} = H\Psi \tag{3.5}$$

$$\vec{v}_k = \frac{\hbar}{m_k}\frac{\Im(\psi^*\nabla_k\psi)}{\psi^*\psi} \tag{3.6}$$

where H is the usual Hamiltonian from the quantum mechanics. The constraints, on the other hand, are as follows:

$$H_{BM} = \sum_k \frac{1}{2}m_k v_k^2 + \frac{1}{2}\sum_{k,k'} V(\vec{r}_k, \vec{r}_{k'}) = 0 \tag{3.7}$$

$$\vec{L}_{BM} = \sum_k m_k \vec{r}_k \times \vec{v}_k = 0 \tag{3.8}$$

$$D_{BM} = \sum_k m_k \vec{r}_k \cdot \vec{v}_k = 0. \tag{3.9}$$

The solutions of Machian Bohmian Mechanics are those that satisfy the equations of motion and the constraints written above.

3.2. Some Example Solutions for Machian Bohmian Mechanics

For illustrative purposes, we consider in this Section particles of the same mass (m).

3.2.1. Single Particle

The solution for a single particle is very straightforward. The wave function is constant and therefore its velocity vanishes. The solution is a single particle at rest at the origin.

3.2.2. Two particles

If the velocity of the first particle is $\vec{v}_1$ then the velocity of the second particle should be:

$$\vec{v}_2 = -\vec{v}_1. \tag{3.10}$$

The motion of particles is on a line. Let that line be the x-axis. The total angular momentum is:

$$\vec{L}_{BM} = m\vec{r}_1 \times \vec{v}_1 + m\vec{r}_2 \times \vec{v}_2 = 0. \tag{3.11}$$

On the other hand, the energy constraint requires $E = mv_1^2 + V(x, -x) = 0$. If there is no interaction among the particles, we need to have $\vec{v}_1 = 0$ and we have two standing particles. If there is interaction, the situation is more complex and the wave function of the particles should be used. This may be a future direction for research.

4. GRAVITATIONAL COLLAPSE OF A SPHERICALLY SYMMETRIC THIN SHELL OF DUST IN SHAPE DYNAMICS

In this Chapter, we follow Ref. [2] closely.

Previously ref. [40] investigated the gravitational collapse of a spherically symmetric thin shell of dust in SD. However the space they used was asymptotically flat and non-compact therefore their result was not exactly satisfactory from a SD perspective. In ref. [2] we investigated the gravitational collapse phenomenon in a compact space without boundary. We now give the details of our calculations in ref. [2]. Readers who are interested in primary sources should consult to ref. [2].

We consider a filled-in ball of coordinate radius 1: $[0,1] \times S^2$ where a spherically symmetric thin shell of dust is located at coordinate radius r_s. See Figure 4.1

The total radial momentum of the shell is p_s. We will consider the metric and its conjugate momentum in the vacuous regions inside and outside the shell. They can be defined most generally as follows [9]:

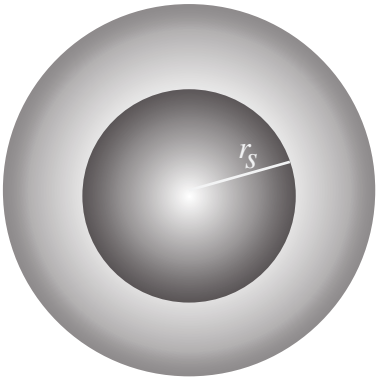

Figure 4.1. The spherically symmetric thin shell of dust is located at radial coordinate r_s in a unit ball ($[0,1] \times S^2$) [2].

$$g_{ab} = \mathrm{diag}(\mu^2, \sigma, \sigma \sin^2\theta) \tag{4.1}$$

$$p^{ab} = \mathrm{diag}\left(\frac{f}{\mu}, \frac{s}{2}, \frac{s}{2\sin^2\theta}\right) \sin\theta \tag{4.2}$$

where μ, σ, f, s, are yet unspecified functions of the radial coordinate r. In the CMC (Constant Mean extrinsic Curvature) gauge, the vacuum SD constraints are as follows [9]:

$$0 = \mathcal{H} = \frac{1}{\sqrt{g}}\left(p^{ab}p_{ab} - \frac{1}{2}p^2\right) - \sqrt{g}R \tag{4.3}$$

$$0 = \mathcal{H}_a = -2\nabla_b p^b_a \tag{4.4}$$

$$0 = p - \sqrt{g}\langle p\rangle \tag{4.5}$$

where $\mathcal{H}$ is the ADM momentum, $\mathcal{H}_a$ is the three dimensional diffeomorphism constraint and p is the trace of the conjugate momentum of the three dimensional metric. When g_{ab} (4.1) and p^{ab} (4.2) are put in equations (4.3), (4.4) and (4.5) we get the following equations [9]:

$$-\frac{1}{6\sigma\mu^2}\Big[\sigma^2\mu s^2 + 4f^2\mu^3 - 4f\sigma\mu^2 s + 12\sigma\mu\sigma'' - 12\sigma\sigma'\mu' - 3\mu(\sigma')^2 - 12\sigma\mu^3 - \langle p\rangle^2\sigma^2\mu^3\Big] = 0 \tag{4.6}$$

$$\mu f' - \frac{1}{2}s\sigma' = 0 \tag{4.7}$$

$$\mu f + s\sigma - \langle p\rangle\mu\sigma = 0 \tag{4.8}$$

where ($'$) means differentiation with respect to r. The use of equations (4.4) and (4.5) yields:

$$f\sqrt{\sigma} - \frac{1}{3}\langle p\rangle\sigma^{3/2} = A \tag{4.9}$$

where A is a constant of integration. When this solution is used in the Hamiltonian constraint we obtain the following:

$$\left(\frac{\sigma'}{\sigma^{1/4}\mu}\right)^2 - 4\sqrt{\sigma} - \frac{f^2}{\sqrt{\sigma}} = -8m. \tag{4.10}$$

Then we put (4.9) into equation (4.10) we obtain the μ^2 as:

$$\mu^2 = \frac{(\sigma')^2}{A^2\sigma^{-1} + (\frac{2}{3}\langle p\rangle A - 8m)\sigma^{1/2} + 4\sigma + \frac{1}{9}\langle p\rangle^2\sigma^2}. \tag{4.11}$$

$(\sigma')^2$ is always nonnegative. Since μ^2 should be always positive, this requirement puts conditions on the denominator appearing in equation (4.11). These conditions are investigated in detail in ref. [9], interested readers should consult to this review.

4.1. Coupling a Thin Shell of Dust to Gravity and the Jump Conditions

In ref. [40], a spherically symmetric thin shell of dust has been coupled to shape dynamics using the following relations:

$$\mathcal{H} = \delta(x^b - y^b)\sqrt{g^{ab}p_a p_b + m_0^2} \tag{4.12}$$

$$\mathcal{H}_a = \delta(x^b - y^b)p_a. \tag{4.13}$$

When the continuum limit of particles on a shell of radius r_s, the constraints become [40]:

$$\mathcal{H} = \sqrt{h}\ \rho(r_s)\ \delta(r - r_s)\ \sqrt{g^{rr}p_r^2 + m_0^2} \tag{4.14}$$

$$\mathcal{H}_a = \delta_a^r\ \sqrt{h}\ \rho(r_s)\ \delta(r - r_s)\ p_r \tag{4.15}$$

where $\rho(r_s)$ is a scalar function yet to be determined and h_{ij} is the metric on S^2 induced by g_{ij}. If we impose that in this process the number of particles is constant, we obtain [40]:

$$\rho(r_s)\int d\theta d\phi\sqrt{h(r_s)} = 4\pi n. \tag{4.16}$$

If the momentum and mass are rescaled as $p_s = np_r$ and $M = nm_0$, the constraints (4.6), (4.7) and (4.8) become [9]:

$$
\begin{aligned}
&- \frac{1}{6\sigma\mu^2}\Big[\sigma^2\mu s^2 + 4f^2\mu^3 - 4f\sigma\mu^2 s + 12\sigma\mu\sigma'' \\
&\quad - 12\sigma\sigma'\mu' - 3\mu(\sigma')^2 - 12\sigma\mu^3 - \langle p\rangle^2\sigma^2\mu^3\Big] \\
&= \delta(r - r_s)\sqrt{p_s^2/\mu^2 + M^2} \qquad (4.17)
\end{aligned}
$$

$$
\mu f' - \frac{1}{2}s\sigma' = -\frac{p_s}{2}\delta(r - r_s) \qquad (4.18)
$$

$$
\mu f + s\sigma - \langle p\rangle\mu\sigma = 0. \qquad (4.19)
$$

The CMC constraint (4.19) gives us $s = \langle p\rangle\mu - \mu f/\sigma$ and when we place it in (4.18) we obtain:

$$
\frac{\mu}{\sqrt{\sigma}}\left(f\sqrt{\sigma} - \frac{1}{2}\langle p\rangle\sigma\right)' = -\frac{p_s}{2}\delta(r - r_s). \qquad (4.20)
$$

The solution of (4.20) is given in [9, 40], and it is as follows:

$$
f(r) = \frac{1}{2}\langle p\rangle\sqrt{\sigma} + \frac{A_-}{\sqrt{\sigma}}\Theta(r_s - r) + \frac{A_+}{\sqrt{\sigma}}\Theta(r - r_s) \qquad (4.21)
$$

where Θ is the Heaviside distribution and

$$
A_+ - A_- = -\frac{p_s\sqrt{\sigma(r_s)}}{2\mu(r_s)} \qquad (4.22)
$$

where A_- and A_+ are functions of r_s and p_s. When we look at (4.17), the only singular part on the left hand side is due to $-2\sigma''/\mu$ and we have [9]:

$$\text{sing}\left(\frac{2\sigma''}{\mu}\right) = -\delta(r - r_s)\sqrt{p_s^2/\mu^2 + M^2} \tag{4.23}$$

which gives

$$\text{sing}(\sigma'') = -\frac{1}{2}\delta(r - r_s)\sqrt{p_s^2 + M^2\mu^2}. \tag{4.24}$$

Let $\gamma = \lim_{r\to r_s^+}\sigma'$ and $\kappa = \lim_{r\to r_s^-}\sigma'$, then we have [9]:

$$\gamma - \kappa = -\frac{1}{2}\sqrt{p_s^2 + M^2\mu^2(r_s)}. \tag{4.25}$$

Now we need to impose the continuity of μ. The use of equation (4.11) yields:

$$\frac{\kappa^2}{A_-^2\sigma^{-1}(r_s) + (\frac{2}{3}\langle p\rangle A_- - 8m_-)\sigma^{1/2}(r_s) + 4\sigma(r_s) + \frac{1}{9}\langle p\rangle^2\sigma^2(r_s)} = \frac{\gamma^2}{A_+^2\sigma^{-1}(r_s) + (\frac{2}{3}\langle p\rangle A_+ - 8m_+)\sigma^{1/2}(r_s) + 4\sigma(r_s) + \frac{1}{9}\langle p\rangle^2\sigma^2(r_s)}. \tag{4.26}$$

In the next section, we investigate the time evolution of the shell.

4.2. Time Evolution of the Shell

In order to obtain the dynamics of the shell, we need to calculate the symplectic form which facilitates the use of Poisson brackets. For that purpose we first introduce the presymplectic form:

$$\theta = \int dr d\theta d\phi p^{ab} \delta g_{ab} + 4\pi p_s \delta r_s. \tag{4.27}$$

When definitions of metric and conjugate momentum of metric (they are defined in (4.1) and (4.2)) are considered and put in equation 4.27 and the angular part is integrated out, we have the following:

$$\theta = 4\pi \int_0^1 dr (2f\delta\mu + s\delta\sigma) + 4\pi p_s \delta r_s. \tag{4.28}$$

We use the CMC condition (4.19) and we find:

$$\theta = 4\pi \int_0^1 dr \left(\langle p \rangle \mu \delta\sigma - \frac{2\mu}{\sqrt{\sigma}} \delta(f\sqrt{\sigma}) \right) + 4\pi p_s \delta r_s. \tag{4.29}$$

We use f that is found in (4.21), and we obtain:

$$\theta = -\underbrace{\frac{8\pi}{3}\int_0^1 dr\mu\sigma\delta\langle p\rangle}_{\equiv\phi} -8\pi\left[\delta A_- \int_0^{r_s} dr\frac{\mu}{\sqrt{\sigma}} + \delta A_+ \int_{r_s}^1 dr\frac{\mu}{\sqrt{\sigma}}\right]. \tag{4.30}$$

Now we use the isotropic coordinates: $\mu = \sqrt{\sigma}/r$. In this case, the presymplectic potential becomes $\theta = -\phi + 8\pi\ \delta(A_+ - A_-)\ln r_s$ modulo an exact form. Using equation (4.22) we can write this as follows:

$$\theta = -\phi - 4\pi\ \delta(p_s r_s)\ln r_s. \tag{4.31}$$

The symplectic form, ω, which is $-\delta\theta$ is found as:

$$\omega = -\delta\theta = \delta\phi + 4\pi\ \delta r_s \wedge \delta p_s. \tag{4.32}$$

Here $\delta\phi$ does not depend on δr_s or δp_s. In matrix form, ω can be represented as follows:

$$\omega_{ab} = \begin{pmatrix} F(\delta\phi) & 0 & 0 \\ 0 & 0 & 4\pi \\ 0 & -4\pi & 0 \end{pmatrix} \tag{4.33}$$

where the order of the coordinates are ordered such that the last two ones are r_s, p_s where F is some function of $\delta\phi$. The inverse of the symplectic form which is required to calculate the Poisson brackets is found as:

$$\omega^{ab} = \begin{pmatrix} F^{-1}(\delta\phi) & 0 & 0 \\ 0 & 0 & -1/4\pi \\ 0 & 1/4\pi & 0 \end{pmatrix}. \tag{4.34}$$

The matrix inverse of the symplectic form, Equation (4.34), can be used the derive the equations of motion for the shell variables.

So far, we have given an outline of a spherically symmetric thin shell of dust under gravitational collapse in Shape Dynamics. We have calculated the symplectic form and its inverse that will be used to derive the equations of motion of the theory using Poisson brackets. We leave the actual details of the dynamics of the shell for a future study.

5. CONCLUSION

In this thesis, we considered a theory of gravitation called Shape Dynamics (SD). The reduced configuration space of Shape Dynamics is the same as that of General Relativity (GR) [7, 8]. However their gauge groups are different: While there is local Lorentz symmetry in GR, there is local scale (Weyl) symmetry in SD. In Chapter 1 we summarized Shape Dynamics.

In Chapter 2 we proved the existence of Unruh effect in 3-torus with a SD background using Bohmian Field Theory. We could not use the machinery of standard Quantum Field Theory (QFT) because it requires Lorentz symmetry which is absent in SD. Because of that reason we used BFT. BFT is a field theory generalization of the well-known Bohmian Mechanics which is a realist interpretation of quantum mechanics. The existence of Unruh effect would normally be unexpected and it is interesting that we proved its existence in a theory that lacks a light-cone structure. This work is published by *The Annals of Physics* [30].

In Chapter 3 we studied the constraints of the particle interaction version of Shape Dynamics (Julian Barbour's Toy Model for Shape Dynamics (JBSD), which is expressed in Appendix B in detail). We wrote down the quantum version of JBSD constraints and imposed them on the particle variables of Bohmian Mechanics. As two examples, we considered a single particle and non-interacting two particle universes. A short version of this work is published by *The Online Journal of Science and Technology* [37].

In Chapter 4 we considered a spherically symmetric thins shell of dust in Shape Dynamics in a space manifold which is $[0, 1] \times S^2$. We calculated the symplectic form and its inverse. The phase space variables turned out to be the coordinate radius and total momentum of the shell, the expectation value of the trace of the metric momentum, and the volume of the space.

All in all, as the title of the thesis tells ("Quantum Phenomena and Shape Dynamics") we tried to do a research on the quantum aspects of SD. By proving the existence of Unruh effect [30] we can say that we did some progress. We also did some interesting research on the unification of Bohmian Mechanics with Mach's Principle. Moreover, we calculated the symplectic form and its inverse for a spherically symmetric thin shell of dust in Shape Dynamics and laid the foundations for future research. It is our hope that this thesis will create a wave of curiosity about Shape Dynamics.

REFERENCES

1. Dündar, F. S., *The Firewall Paradox*, Master's Thesis, Middle East Technical University, Aug. 2014, arXiv:1409.0474.

2. Dündar, F. S., Z. Mirzaiyan and M. Arık, "Gravitational collapse of thin shell of dust in shape dynamics", to be published.

3. Barbour, J., *Quantum Field Theory and Gravity: Conceptual and Mathematical Advances in the Search for a Unified Framework*, chap. Shape Dynamics. An Introduction, pp. 257–297, Springer Basel, Basel, 2012, arXiv:1105.0183.

4. Anderson, E., J. Barbour, B. Z. Foster, B. Kelleher and N. Ó. Murchadha, "The physical gravitational degrees of freedom", *Classical and Quantum Gravity*, Vol. 22, pp. 1795–1802, May 2005.

5. Anderson, E., J. Barbour, B. Foster and N. Ó Murchadha, "Scale-invariant gravity: geometrodynamics", *Classical and Quantum Gravity*, Vol. 20, pp. 1571–1604, Apr. 2003, arXiv:gr-qc/0211022.

6. Barbour, J. and N. O. Murchadha, "Classical and Quantum Gravity on Conformal Superspace", *ArXiv General Relativity and Quantum Cosmology e-prints*, Nov. 1999, arXiv:gr-qc/9911071.

7. Gomes, H., S. Gryb and T. Koslowski, "Einstein gravity as a 3D conformally invariant theory", *Classical and Quantum Gravity*, Vol. 28, No. 4, p. 045005, Feb. 2011, arXiv:1010.2481.

8. Gomes, H. and T. Koslowski, "The link between general relativity and shape dynamics", *Classical and Quantum Gravity*, Vol. 29, No. 7, p. 075009, Apr. 2012, arXiv:1101.5974.

9. Mercati, F., "A Shape Dynamics Tutorial", *ArXiv e-prints*, Aug. 2014, arXiv:1409.0105.

10. Dürr, D., "Proceedings for the Ischia 1999 conference", Springer-Verlag, 2001.

11. Bell, J., *Speakable and unspeakable in quantum mechanics*, Cambridge University Press, 1987.

12. Goldstein, S., *Physics Today*, Vol. 51, pp. 42–47, 1998.

13. Goldstein, S., *Physics Today*, Vol. 51, pp. 38–42, 1998.

14. Dürr, D., S. Goldstein, R. Tumulka and N. Zanghi, "Trajectories and particle creation and annihilation in quantum field theory", *Journal of Physics A Mathematical General*, Vol. 36, pp. 4143–4149, Apr. 2003, arXiv:quant-ph/0208072.

15. Dürr, D., S. Goldstein, R. Tumulka and N. Zanghi, "Bohmian Mechanics and Quantum Field Theory", *Physical Review Letters*, Vol. 93, No. 9, p. 090402, Aug. 2004, arXiv:quant-ph/0303156.

16. Dürr, D., S. Goldstein, R. Tumulka and N. Zangh, "Quantum Hamiltonians and Stochastic Jumps", *Communications in Mathematical Physics*, Vol. 254, pp. 129–166, Feb. 2005, arXiv:quant-ph/0303056.

17. Dürr, D., S. Goldstein, R. Tumulka and N. Zanghi, "Topical review: Bell-type quantum field theories", *Journal of Physics A Mathematical General*, Vol. 38, pp. R1–R43, Jan. 2005, arXiv:quant-ph/0407116.

18. Colin, S., T. Durt and R. Tumulka, "On Superselection Rules in Bohm-Bell Theories", *ArXiv e-prints*, Sep. 2005, arXiv:quant-ph/0509177.

19. Tumulka, R., "On spontaneous wave function collapse and quantum field theory", *Proceedings of the Royal Society of London Series A*, Vol. 462, pp. 1897–1908, Jun. 2006, arXiv:quant-ph/0508230.

20. Colin, S. and W. Struyve, "A Dirac sea pilot-wave model for quantum field theory", *Journal of Physics A Mathematical General*, Vol. 40, pp. 7309–7341, Jun. 2007, arXiv:quant-ph/0701085.

21. Struyve, W., "Pilot-wave theory and quantum fields", *Reports on Progress in Physics*, Vol. 73, No. 10, p. 106001, Oct. 2010, arXiv:0707.3685.

22. Struyve, W., "Pilot-wave approaches to quantum field theory", *Journal of Physics Conference Series*, Vol. 306 of *Journal of Physics Conference Series*, p. 012047, Jul. 2011, arXiv:1101.5819.

23. Gourgoulhon, E., "3+1 Formalism and Bases of Numerical Relativity", *ArXiv General Relativity and Quantum Cosmology e-prints*, Mar. 2007, arXiv:gr-qc/0703035, 2007.

24. Gomes, H., "A Birkhoff theorem for shape dynamics", *Classical and Quantum Gravity*, Vol. 31, No. 8, p. 085008, Apr. 2014, arXiv:1305.0310.

25. Susskind, L., L. Thorlacius and J. Uglum, "The stretched horizon and black hole complementarity", *Physical Review D*, Vol. 48, pp. 3743–3761, Oct. 1993.

26. Almheiri, A., D. Marolf, J. Polchinski and J. Sully, "Black holes: complementarity or firewalls?", *Journal of High Energy Physics*, Vol. 2, p. 62, Feb. 2013.

27. Page, D. N., "Information in black hole radiation", *Physical Review Letters*, Vol. 71, pp. 3743–3746, Dec. 1993.

28. Susskind, L., "The Transfer of Entanglement: The Case for Firewalls", *ArXiv e-prints*, Oct. 2012, arXiv:1210.2098, 2012.

29. Gomes, H. and G. Herczeg, "A rotating black hole solution for shape dynamics", *Classical and Quantum Gravity*, Vol. 31, No. 17, p. 175014, Sep. 2014.

30. Dündar, F. S. and M. Arık, "Bohmian field theory on a shape dynamics back-

ground and Unruh effect", *Annals of Physics*, Vol. 392, pp. 157 – 164, 2018, arXiv:1706.05890.

31. Unruh, W. G., "Notes on black-hole evaporation", *Physical Review D*, Vol. 14, p. 870, 1976.

32. Copeland, E., P. Davies and K. Hinton, "Acceleration radiation in a compact space", *Classical and Quantum Gravity*, Vol. 1, No. 2, p. 179, 1984.

33. Koslowski, T., "The shape dynamics description of gravity", *Canadian Journal of Physics*, Vol. 93, pp. 956–962, Sep. 2015, arXiv:1501.03007.

34. Green, C. C. and J. S. Marshall, "Green's function for the Laplace–Beltrami operator on a toroidal surface", *Proceedings of the Royal Society of London A: Mathematical, Physical and Engineering Sciences*, Vol. 469, No. 2149, 2012.

35. Chiou, D.-W., "Response of the Unruh-DeWitt detector in flat spacetime with a compact dimension", *Physical Review D*, Vol. 97, p. 124028, June 2018, arXiv:1605.06656.

36. Hodgkinson, L., *Particle detectors in curved spacetime quantum field theory*, Ph.D. Thesis, University of Nottingham, October 2013, arXiv:1309.7281.

37. Dündar, F. S. and M. Arık, "Bohmian Mechanics made Machian", *The Online Journal of Science and Technology*, Vol. 8, pp. 26–28.

38. Bondi, H. and J. Samuel, "The Lense-Thirring effect and Mach's principle", *Physics Letters A*, Vol. 228, pp. 121–126, Feb. 1997.

39. Barbour, J., "The Definition of Mach's Principle", *Foundations of Physics*, Vol. 40, No. 9, pp. 1263–1284, 2010, arXiv:1007.3368.

40. Mercati, F., H. Gomes, T. Koslowski and A. Napoletano, "Gravitational collapse of thin shells of dust in asymptotically flat shape dynamics", *Phys. Rev. D*, Vol. 95,

p. 044013, Feb 2017, arXiv:1509.00833.

41. Birrell, N. D. and P. C. W. Davies, *Quantum Fields in Curved Space*, Cambridge University Press, 1982.

APPENDIX A: THE STANDARD UNRUH RADIATION

We now give the standard derivation of the Unruh effect in $1+1$ flat spacetime. In what follows, we use ref. [1]. We will show the existence of Unruh radiation for a massless scalar field. The field equation is $\nabla^2\phi = 0$. The metric is $g_{\mu\nu} = \mathrm{diag}(-1, 1)$.In Minkowski space this reduces to the following equation:

$$-\partial_t^2\phi + \partial_x^2\phi = 0. \tag{A.1}$$

The positive frequency solutions are given by $f_k^{\mathrm{in}} = \exp(-i\omega t + ikx)$ where $\omega = |k|$. If a solution f is positive frequency, it means that the Lie derivative of f along time direction equals $-i\omega f$ for a positive ω. The negative frequency solutions are complex conjugates of positive frequency solutions. The normalized f_k^{in} is as follows:

$$f_k^{\mathrm{in}} = (4\pi\omega)^{-1/2} e^{-i\omega t + ikx}. \tag{A.2}$$

We now are in a position to define Rindler coordinates [1] (see Figure A.1):

$$t_{\mathrm{L}} = -\frac{1}{a} e^{a\xi} \sinh(a\eta) \qquad x_{\mathrm{L}} = -\frac{1}{a} e^{a\xi} \cosh(a\eta) \tag{A.3}$$

$$t_{\mathrm{R}} = \frac{1}{a} e^{a\xi} \sinh(a\eta) \qquad x_{\mathrm{R}} = \frac{1}{a} e^{a\xi} \cosh(a\eta) \tag{A.4}$$

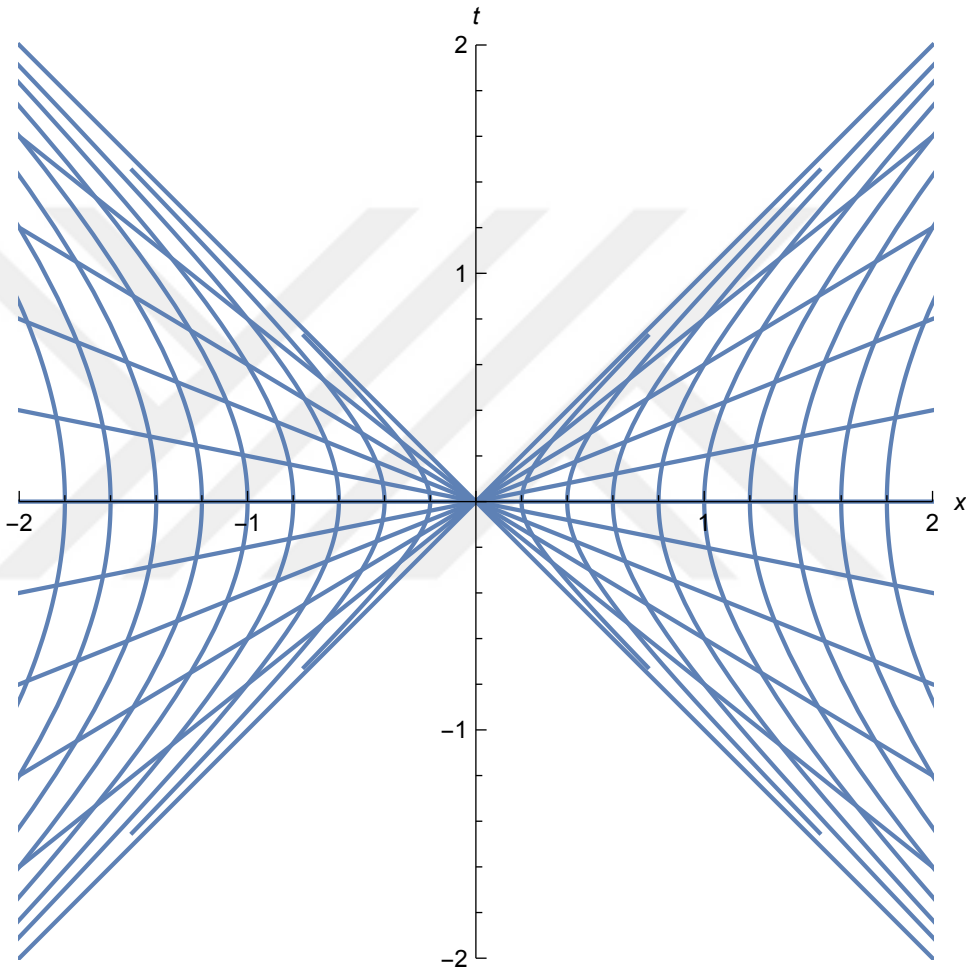

Figure A.1. Hyperbolas on the left and right Rindler wedges are the worldlines of observers with constant acceleration a and are parametrized with ξ. The lines passing through the origin mark the constant time surfaces that accelerated observers experience and are parametrized with η.

In Rindler coordinates the metric is found out to be the following [1]:

$$ds^2 = e^{2a\xi}(-d\eta^2 + d\xi^2) \tag{A.5}$$

and the non-vanishing Christoffel symbols are:

$$\Gamma^{\xi}_{\xi\xi} = \Gamma^{\xi}_{\eta\eta} = \Gamma^{\eta}_{\eta\xi} = a. \tag{A.6}$$

The field equation is $\nabla^2\phi = g^{\mu\nu}\partial_\mu\phi\partial_\nu\phi - g^{\mu\nu}\Gamma^{\lambda}_{\mu\nu}\partial_\lambda\phi = 0$. Since the metric is diagonal with temporal and spatial part equal in magnitude but with opposite signs, the contribution from the Christoffel symbol cancels out and we are left with the following: $e^{-2a\xi}(-\partial^2_\eta + \partial^2_\xi)\phi = 0$. Since the factor in front of the differential operator never vanishes we have:

$$-\partial^2_\eta\phi + \partial^2_\xi\phi = 0. \tag{A.7}$$

Here the solutions are given as $\exp(\pm i\omega\eta + ik\xi)$. However there is a subtlety. In the right Rindler wedge ∂_η is the time-like Killing vector, however in the left Rindler wedge $-\partial_\eta$ is the time-like Killing vector. Therefore the normalized positive frequency solutions in the left and right Rindler wedges are given as follows [1]:

$$f_k^{\mathrm{L}} = (4\pi\omega)^{-1/2} e^{i\omega\eta + ik\xi} \tag{A.8}$$

$$f_k^{\mathrm{R}} = (4\pi\omega)^{-1/2} e^{-i\omega\eta + ik\xi}. \tag{A.9}$$

These functions are normalized according to the $U(1)$-inner-product given in the left and right Rindler wedges as follows [1]:

$$(\phi, \psi)_{\mathrm{L,R}} = \pm i \int_{\mathrm{const.}\eta} d\xi (\psi \partial_\eta \phi^* - \phi^* \partial_\eta \psi). \tag{A.10}$$

We want to know how many quanta are there in the Rindler vacuum when the field is in the Minkowski vacuum. For that purpose, we could immediately go on to calculate the Bogoluibov coefficients however there is a more elegant method by Unruh [31]. Ref. [41] gives the following two normalized positive frequency solutions constructed out of mode solutions in left and right Rindler wedges, which are analytic in the Minkowski space-time:

$$f_k^{(1)} = \frac{e^{\pi\omega/2a} f_k^{\mathrm{R}} + e^{-\pi\omega/2a} f_{-k}^{\mathrm{L},*}}{[2\sinh(\pi\omega/a)]^{1/2}} \quad f_k^{(2)} = \frac{e^{-\pi\omega/2a} f_{-k}^{\mathrm{R},*} + e^{\pi\omega/2a} f_k^{\mathrm{L}}}{[2\sinh(\pi\omega/a)]^{1/2}}. \tag{A.11}$$

We can expand the field into field modes in two ways:

$$\phi = \int dk (f_k^{(1)} a_k^{(1)} + f_k^{(1),*} a_k^{(1),\dagger} + f_k^{(2)} a_k^{(2)} + f_k^{(2),*} a_k^{(2),\dagger}) \tag{A.12}$$

where $a_k^{(1)}, a_k^{(2)}$ annihilate the Minkowski vacuum $|M\rangle$, and

$$\phi = \int dk (f_k^{\mathrm{L}} a_k^{\mathrm{L}} + f_k^{\mathrm{L},*} a_k^{\mathrm{L},\dagger} + f_k^{\mathrm{R}} a_k^{\mathrm{R}} + f_k^{\mathrm{R},*} a_k^{\mathrm{R},\dagger}). \tag{A.13}$$

By replacing the definition of $f_k^{(1)}, f_k^{(2)}$ in (A.11) into (A.12) and rearranging the terms we obtain:

$$a_k^{\mathrm{L}} = \frac{e^{-\pi\omega/2a} a_{-k}^{(1),\dagger} + e^{\pi\omega/2a} a_k^{(2)}}{[2\sinh(\pi\omega/a)]^{1/2}} \quad a_k^{\mathrm{R}} = \frac{e^{\pi\omega/2a} a_k^{(1)} + e^{-\pi\omega/2a} a_{-k}^{(2),\dagger}}{[2\sinh(\pi\omega/a)]^{1/2}}. \tag{A.14}$$

Using (A.14) we obtain:

$$\langle M | a_k^{\mathrm{L},\dagger} a_k^{\mathrm{L}} | M \rangle = \langle M | a_k^{\mathrm{R},\dagger} a_k^{\mathrm{R}} | M \rangle = \frac{\delta(0)}{e^{2\pi\omega/a} - 1}. \tag{A.15}$$

The appearance of Dirac delta function is due to use of continuous parameter k. For that purpose we construct wave-packets as follows [1]:

$$g_{jn}^{\mathrm{L,R}} \equiv \varepsilon^{-1/2} \int_{j\varepsilon}^{(j+1)\varepsilon} dk e^{-i2\pi nk/\varepsilon} f_k^{\mathrm{L,R}} \tag{A.16}$$

and the field can be expanded into these modes:

$$\phi = \sum_{jn} \left(g^{\mathrm{L}}_{jn} b^{\mathrm{L}}_{jn} + g^{\mathrm{L},*}_{jn} b^{\mathrm{L},\dagger}_{jn} + g^{\mathrm{R}}_{jn} b^{\mathrm{R}}_{jn} + g^{\mathrm{R},*}_{jn} b^{\mathrm{R},\dagger}_{jn} \right). \tag{A.17}$$

We provide the result of expectation value of number operators in the left and right Rindler wedges (for more details consult to [1]):

$$\langle M | b^{\mathrm{L},\dagger}_{jn} b^{\mathrm{L}}_{jn} | M \rangle = \langle M | b^{\mathrm{R},\dagger}_{jn} b^{\mathrm{R}}_{jn} | M \rangle = \varepsilon^{-1} \int_{j\varepsilon}^{(j+1)\varepsilon} dk \frac{1}{e^{2\pi\omega/a} - 1}. \tag{A.18}$$

In the limit $\varepsilon \ll 1$, we obtain:

$$\langle M | b^{\mathrm{L},\dagger}_{jn} b^{\mathrm{L}}_{jn} | M \rangle = \langle M | b^{\mathrm{R},\dagger}_{jn} b^{\mathrm{R}}_{jn} | M \rangle = \frac{1}{e^{2\pi\omega/a} - 1}. \tag{A.19}$$

This is the finite result we are interested in. It means that the observer sees a blackbody spectrum with temperature $T = a/2\pi$. The more accelerated the observer is, the more hotter the radiation becomes.

APPENDIX B: JULIAN BARBOUR'S TOY MODEL FOR SHAPE DYNAMICS

We begin with N point particles interacting through a potential V. There is a restriction on N such that it should be greater than or equal to three. This is because a single point can be made static by moving to its center of mass frame. Two particles also do not form a *shape* because the distance between them can be mapped to any value through a scale transformation. Julian Barbour's toy model of SD (in short JBSD) [3] begins with three particles. In this Appendix, we follow the notation of Barbour [3]. Ref. [9] is a review of SD including this toy model; readers may also consult to this reference.

Let r_{ab} be the distance between the particle a and particle b. We need a way to obtain dimensionless quantities out of r_{ab} and it is obtained as follows [3]:

$$\tilde{r}_{ab} = \frac{r_{ab}}{R_{rmh}}, \quad R_{rmh} \equiv \left[\sum_{a<b} r_{ab}^2\right]^{1/2}. \tag{B.1}$$

Here R_{rmh} is the "root-mean-harmonic separation" [3]. r_{ab} is our *physical* data to be considered. Therefore, only the angles between particles are of physical importance. See Figure B.1 and Figure B.2.

In JBSD, translations (T), rotations (R) and global scale transformations (S) are pure gauge. The set of all Cartesian configuration of N particles is denoted by Q^N. The shape space is defined as the quotient space of Q^N by the group of all gauge transformations: $Q_S \equiv Q^N/TRS$.

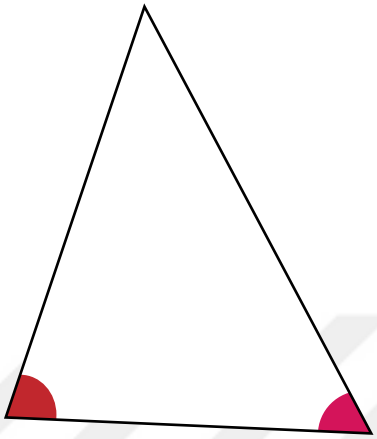

Figure B.1. In a three particle system, the physical quantities are the two angles of the triangle formed by the particles.

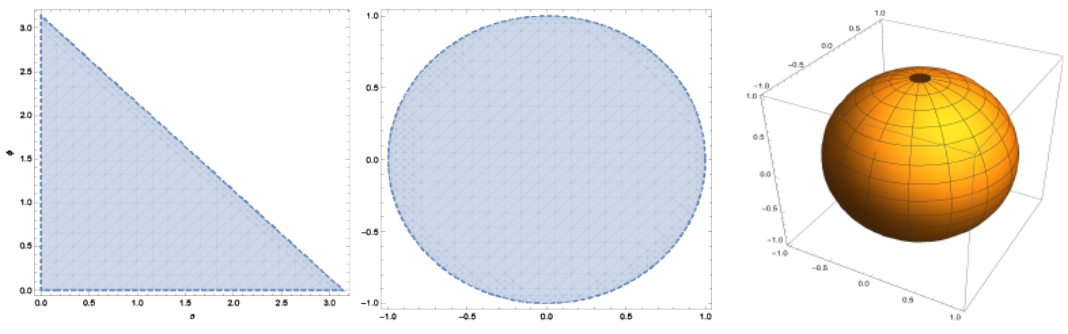

Figure B.2. There are two physically relevant coordinates (angles) of a three particle configuration. They can be represented on a sphere whose north-pole is removed.

According to Julian Barbour's interpretation of Mach's Principle [39] SD satisfies the strong form of Mach's Principle: a point in reduced configuration space (*i.e.* shape space) and a direction (a vector of unit magnitude) determines the evolution of the system uniquely. See Figure B.3.

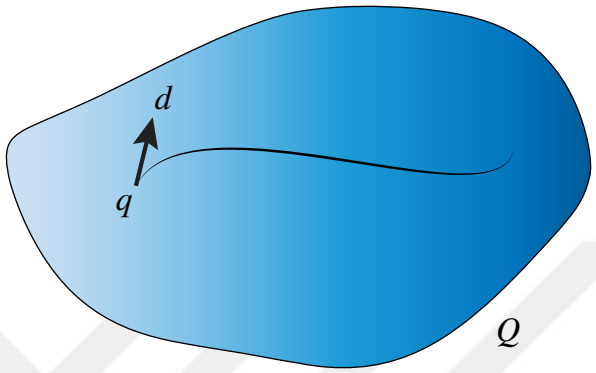

Figure B.3. A point (q) in reduced configuration space (Q) and a direction (d) or a tangent vector determines the time evolution of the system uniquely.

Let $\vec{x}_a$ be the position of the particle-a in the Cartesian space, *i.e.* $\mathbb{R}^3$. In JBSD we have a kinematic metric:

$$T_{kin} \equiv \frac{1}{2} \sum_a m_a \frac{d\vec{x}_a}{d\lambda} \cdot \frac{d\vec{x}_a}{d\lambda} \tag{B.2}$$

where λ is an arbitrary parameter used instead of Newtonian time.

Let E be some constant (will be determined later) and V be the potential function. Then by requiring the following functional to have a zero variation [3]:

$$\delta I = 0, \quad I \equiv 2 \int d\lambda \left[(E - V) T_{kin} \right]^{1/2} \tag{B.3}$$

we can obtain the equations of motion as follows:

$$\frac{d}{d\lambda}\left(\sqrt{\frac{E-V}{T_{kin}}}m_a\frac{d\vec{x}_a}{d\lambda}\right) = -\sqrt{\frac{T_{kin}}{E-V}}\frac{\partial V}{\partial \vec{x}_a} \tag{B.4}$$

where there is no summation on a. We can make a transformation on $\lambda \to t$ such that $E - V = T_{kin}$ we obtain the Newtonian equations of motion:

$$m_a\frac{d^2\vec{x}_a}{dt^2} = -\vec{\nabla}_a V. \tag{B.5}$$

The differential of the parameter t (that is, the Newtonian absolute time) is given by [3]:

$$dt = \left[\frac{\sum_a m_a d\vec{x}_a \cdot d\vec{x}_a}{2(E-V)}\right]^{1/2}. \tag{B.6}$$

As it can be seen on equation (B.6), dt can only be determined by summation over the whole space. Therefore the Newtonian absolute time is seen to be a *holistic* time.

There is also the concept of *best-matching*: Best-matching of shapes is done by fixing one shape and applying gauge transformations to the second shape and finding the difference between them. The following is the best-matching distance between the two shapes (let the coordinates of the first shape be $\vec{x}_a$ and the second one be $\vec{x}'_a$) [9]:

$$d_{bm} \equiv \inf_{\vec{\theta},\Omega,\phi} \sum_a |\vec{x}_a - \phi\Omega\vec{x}'_a - \vec{\theta}| \tag{B.7}$$

where $\phi \in \mathbb{R}^+, \Omega \in SO(3)$ and $\vec{\theta} \in \mathbb{R}^3$. See Figure B.4.

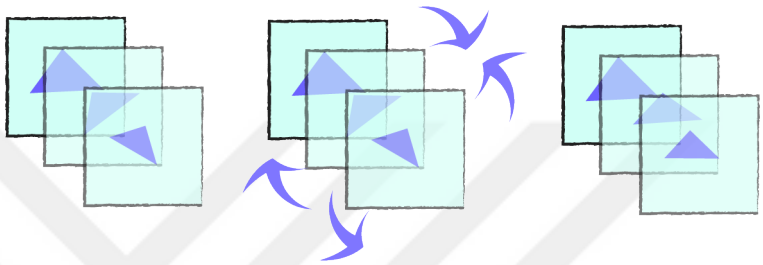

Figure B.4. The best-matched distance between shapes is found out as fixing one shape and applying gauge transformations to the second shape and minimizing equation (B.7).

By choosing the gauge transformations properly, we can always ensure that the total momentum, total angular momentum and the total dilational momentum of the system vanishes [3]:

$$\vec{P} = \sum_a \vec{p}_a = 0 \tag{B.8}$$

$$\vec{L} = \sum_a \vec{x}_a \times \vec{p}_a = 0 \tag{B.9}$$

$$D = \sum_a \vec{x}_a \cdot \vec{p}_a = 0. \tag{B.10}$$

Therefore a configuration in the shape space has $3N - 7$ many coordinates. As it is seen in equation (B.7) the first shape is fixed, and the minimum distance between the two shapes is found out by applying scale transformation (ϕ), rotations (Ω) and translations ($\vec{\theta}$) to the second shape. See Figure B.5. By using the best-matched dis-

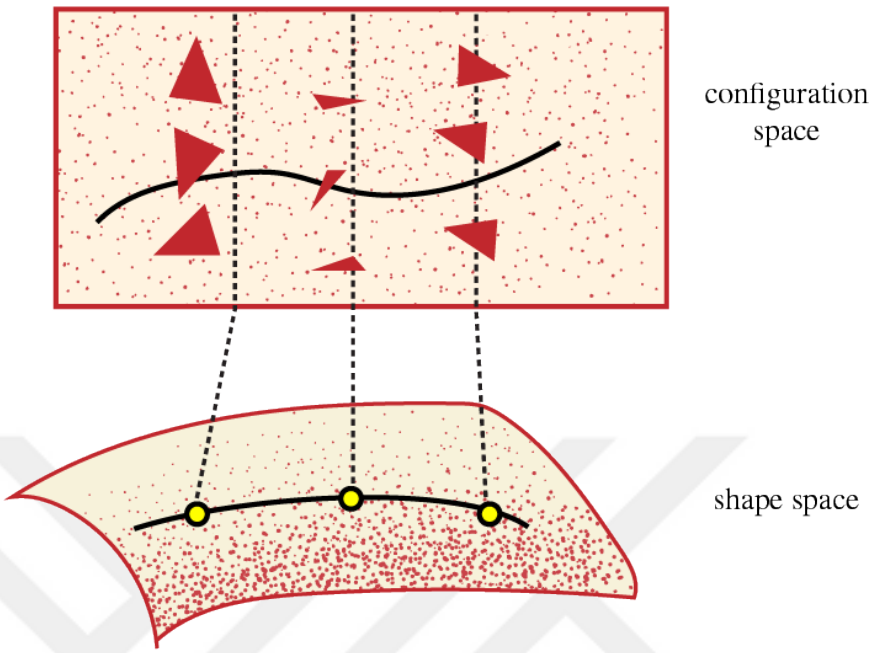

Figure B.5. The best-matched distance between two shapes is found in the configuration space. Thus a unique curve in reduced configuration space (*i.e.* shape space) is determined.

tance between two shapes, a dynamics in the shape space can be defined [9]. Moreover the total energy of the system should vanish because it is a dimensionful quantity, $E = 0$ [3]. Hence, JBSD has a purely relational description in the shape space.

APPENDIX C: THE DERIVATION OF THE PROBABILITY CURRENT

In this Appendix, we will derive the probability current in quantum mechanics. We will begin with the Schrödinger equation and its complex conjugate:

$$i\hbar\partial_t\Psi = -\frac{\hbar^2}{2m}\nabla^2\Psi + V\Psi \tag{C.1}$$

$$-i\hbar\partial_t\Psi^* = -\frac{\hbar^2}{2m}\nabla^2\Psi^* + V\Psi^*. \tag{C.2}$$

Now multiply the first equation by Ψ^* and the second one by Ψ:

$$i\hbar\Psi^*\partial_t\Psi = -\frac{\hbar^2}{2m}\Psi^*\nabla^2\Psi + V|\Psi|^2 \tag{C.3}$$

$$-i\hbar\Psi\partial_t\Psi^* = -\frac{\hbar^2}{2m}\Psi\nabla^2\Psi^* + V|\Psi|^2. \tag{C.4}$$

We subtract the second equation from the first one, and obtain:

$$i\hbar(\Psi^*\partial_t\Psi + \Psi\partial_t\Psi^*) = -\frac{\hbar^2}{2m}(\Psi^*\nabla^2\Psi - \Psi\nabla^2\Psi^*). \tag{C.5}$$

We can write this equation as a continuity equation as follows:

$$\partial_t |\Psi|^2 + \vec{\nabla} \cdot \vec{j} = 0 \tag{C.6}$$

where

$$\vec{j} = \frac{\hbar}{2im}(\Psi^* \vec{\nabla} \Psi - \Psi \vec{\nabla} \Psi^*) \tag{C.7}$$

and $\vec{j}$ is called as the "probability current." We can also write it as follows:

$$\vec{j} = \frac{\hbar}{m} \Im(\Psi^* \vec{\nabla} \Psi) \tag{C.8}$$

where $\Im(\cdot)$ denotes the imaginary part of the term inside the parenthesis.